Optics Communications 283 (2010) 2849–2856

Contents lists available at ScienceDirect

Optics Communications

journal homepage: www.elsevier.com/locate/optcom

Optical spectra of graded nanostructured TiO_2 chiral sculptured thin films

F. Babaei [a], A. Esfandiar [b], H. Savaloni [b,*]

[a] Department of Physics, University of Qom, Qom, Iran
[b] Department of Physics, University of Tehran, North-Kargar Street, Tehran, Iran

ARTICLE INFO

Article history:
Received 15 August 2009
Received in revised form 7 February 2010
Accepted 6 March 2010

Keywords:
Graded chiral thin films
Oblique-angle deposition
Circular selectivity

ABSTRACT

The optical properties of graded chiral sculptured TiO_2 thin films in axial and non-axial excited states are calculated using the rigorous coupled wave analysis method (RCWA) in conjunction with the Bruggeman homogenization formalism. The filtering frequency and polarization selectivity of these graded nanostructured TiO_2 sculptured thin films showed dependence on both structural and deposition parameters. The results achieved are consistent with the experimental data [K. M. Krause and M. J. Bret, Adv. Funct. Mater. 18 (2008) 3111].

1. Introduction

Chiral thin films or chiral sculptured thin films (CSTFs) are columnar (range between 1 and 100 nm) thin films deposited on substrate with a tilt angle, α, by a method known as oblique-angle deposition (OAD) and controlled azimuthal rotation, φ of the substrate. The columnar structure of thin film can be designed in nano and micro scale 3D for use in optical, chemical, mechanical, biological, electrical and magnetic applications [1]. The above mentioned method can be used to produce 3D photonic crystals that depending on their nano-structural dimensions they prohibit the propagation of a certain bands of electromagnetic frequency through macroscopic (Bragg) and microscopic scattering resonances [2].

The most important optical feature of chiral sculptured thin films is the circular Bragg phenomenon that unlike ordinary thin films occurs in chiral sculptured thin films. This phenomenon is studied extensively both theoretically [3–11] and experimentally [12–15]. If the handedness of the chiral sculptured thin film is the same as that of the polarization of the incident circular plane wave, then nearly all the incident light will be reflected in a narrow region of the wavelength (this is called the Bragg regime), otherwise nearly all the incident light will be transmitted. In these films (chiral sculptured thin films grown normal to the substrate surface) the helical axis or the axis of non-homogeneity is normal to the substrate surface (z-axis). These films can be used to discriminate the right-handed circular polarization (RCP) from the left-handed circular polarization (LCP). There is another group of chiral sculptured thin films called slanted chiral sculptured thin films in which the helical axis is tilted with respect to the normal to the substrate surface. In this kind of thin films due to the periodicity of structural parameters in both normal and parallel directions to the substrate surface, the interaction between circular Bragg phenomenon (specular diffraction) and non-specular diffraction (Rayliegh-Wood anomalies) occurs which can be related to the diffraction gratings [16–19]. The study on the slanted chiral sculptured thin films is of importance in understanding the optical ray diffraction by sculptured thin films [20]. In addition, many applications have been proposed for slanted chiral sculptured thin films, such as optical beam splitters, couplers, nano-band and sub nano-band spectral-hole filters and biosensors [21–24].

A third group of chiral sculptured thin films has been introduced by Krause and Brett [25], so called graded chiral sculptured thin films which are similar to the slanted chiral sculptured thin films with a gradient in their thickness in their nano-column structural assembly (Fig. 1). The graded chiral sculptured thin films are produced using selected fixed oblique deposition angles with a shadowing block positioned at the center of the rotating substrate. This shadowing object modulates the microscopic structure of the thin film and produces spatially graded chiral sculptured thin film with graded optical properties. In these films it is possible to distinguish both polarization and frequency selection simultaneously. This technique can be used to produce polarization responsive and tunable frequency optical filters, sources, and detectors for applications such as multichannel light wave systems as well as providing a graded scaffolding to support liquid crystals [25].

Optical devices with tunable optical functions (refractive index, absorption and extinction coefficient, optical activity and other functions) have always been of interest and desire in different areas

* Corresponding author. Tel.: +98 21 6635776; fax: +98 21 88004781.
E-mail address: savaloni@khayam.ut.ac.ir (H. Savaloni).

0030-4018/$ – see front matter © 2010 Elsevier B.V. All rights reserved.
doi:10.1016/j.optcom.2010.03.005

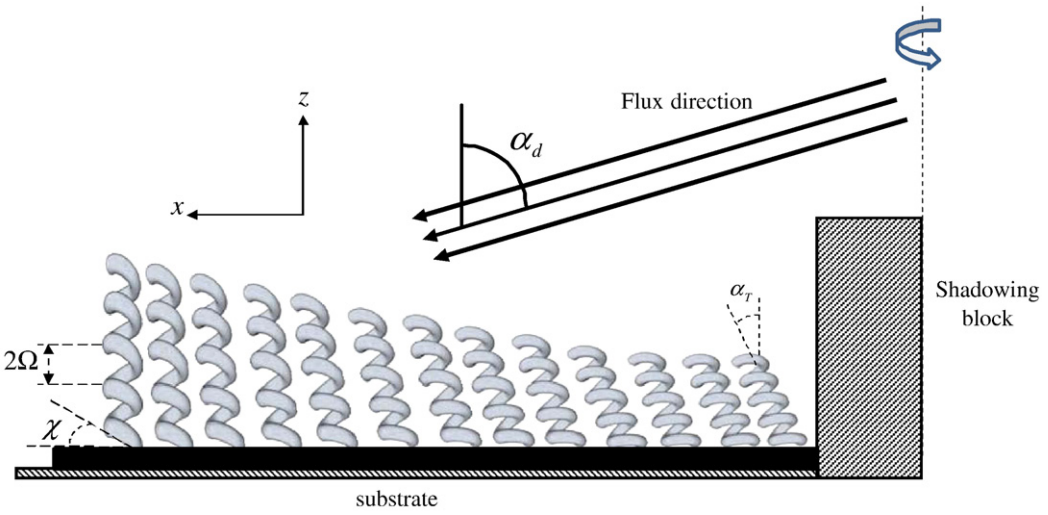

Fig. 1. Schematic of graded nanostructured chiral thin films. α_d, α_T, Ω and χ, are deposition angle, tilt angle, half structural period and rise angle, respectively.

of science and industry. A large body of the recent research in the field of thin films and nano-structures is devoted to the production of optical devices with filtering frequency [26,27 and references therein] and polarization selectivity properties [28 and references therein]. However building of a device, that can have both of these properties simultaneously have been a difficult task. Similar films exist in the nature, such as animals with skins, feathers, wings of varying thickness and chiral structure which while shows different colors it also changes the polarization of the incident light [29–31]. Thin films with variable structural characteristics and filtering frequency at varying frequency along their length have already been produced using different techniques [32–35]. Bragg reflection from gratings is also a method for producing optical components with tuneable characteristics [36,37]. Cunningham et al. [33] also reported a guided-mode resonance filter (GMRF) photonic crystal which can separate the reflection of specific wavelength bands across the width of the component. On the other hand, liquid crystals with helical molecular structures can distinguish the circular polarization of the incident light [38]. Production of nano-structures with sensitivity to the circular polarization of the incident light has also been achieved by means of OAD with azimuthal rotation, φ of the substrate in recent years. Krause and Brett [25] who inspired from the nature used the above combination of OAD and substrate azimuthal rotation as well as fixing a macroscopically shadowing block in the center of the rotating substrate holder to produce thin films with both frequency filtering property and sensitivity to the polarization of the light.

In this work the rigorous coupled wave analysis (RCWA) proposed and extended by Lakhtakia [20] for slanted chiral sculptured thin films is applied to graded chiral sculptured thin films using a computer code written in Mathematica 5.2. Reflection, transmission and circular polarization selectivity for graded chiral sculptured thin films are calculated and compared with the experimental results reported in Ref. [25]. A good agreement between our theoretical results and those of Krause and Brett is achieved.

In Section 2 the finalized formalism of the rigorous coupled wave analysis is given. The numerical results are reported, discussed and compared with Krause and Brett's experimental results in Section 3.

2. Theory

The rigorous coupled wave analysis (RCWA) method was first proposed by Moharam and Gaylord in 1981 [39] in order to obtain a near-exact solution to Maxwell equations for periodic diffracting structures. Wang and Lakhtakia [20] formalized the rigorous coupled wave analysis for the slanted chiral sculptured thin films and obtained the following final algebraic equation:

$$\begin{bmatrix} e^{-id\left[\underline{\tilde{D}}_1\right]}\left[\underline{U}_T\right]\left[\underline{U}_R\right] \\ \left[\underline{V}_T\right]e^{id\left[\underline{\tilde{D}}_2\right]}\left[\underline{V}_R\right] \end{bmatrix}\begin{bmatrix}\left[\underline{T}\right] \\ \left[\underline{R}\right]\end{bmatrix} = \begin{bmatrix}\left[\underline{U}_A\right] \\ e^{id\left[\underline{\tilde{D}}_2\right]}\left[\underline{V}_A\right]\end{bmatrix}\left[\underline{A}\right] \tag{1}$$

where,

$$[\underline{A}] = \begin{bmatrix} a_L^{(n)} \\ a_R^{(n)} \end{bmatrix}, [\underline{R}] = \begin{bmatrix} r_L^{(n)} \\ r_R^{(n)} \end{bmatrix}, [\underline{T}] = \begin{bmatrix} t_L^{(n)} \\ t_R^{(n)} \end{bmatrix} \tag{2}$$

where, $\{a_L^{(n)}, a_R^{(n)}\}$, $\{r_L^{(n)}, r_R^{(n)}\}$, $\{t_L^{(n)}, t_R^{(n)}\}$ are the nth order harmonic complex amplitudes of the incident, and reflection and transmission of left- and right-handed circularly polarized light, respectively. The rest of the parameters in Eq. (1) are described in detail in Section 2-2 of reference [20].

Once all $\{a_L^{(n)}, a_R^{(n)}\}$, $\{r_L^{(n)}, r_R^{(n)}\}$, $\{t_L^{(n)}, t_R^{(n)}\}$ for all n orders have been determined using the RCWA, the nth order reflection and transmission coefficient can be obtained from:

$$r_{\sigma\sigma'} = \frac{r_\sigma^{(n)}}{a_{\sigma'}^{(0)}},\ t_{\sigma\sigma'} = \frac{t_\sigma^{(n)}}{t_{\sigma'}^{(0)}},\ \sigma,\sigma' = L,R \tag{3}$$

The nth order harmonic reflection and transmission are:

$$R_{\sigma\sigma'}^n = \frac{Re\left[k_z^{(n)}\right]}{Re\left[k_z^{(0)}\right]}\left|r_{\sigma\sigma'}^{(n)}\right|^2,\ T_{\sigma\sigma'}^n = \frac{Re\left[k_z^{(n)}\right]}{Re\left[k_z^{(0)}\right]}\left|t_{\sigma\sigma'}^{(n)}\right|^2,\ \sigma,\sigma' = L,R \tag{4}$$

The first subscript shows the polarization state of the reflected or transmitted and the second subscript indicates the polarization state of incident light and Re[ ] is the real part. $k_z^{(n)}$ is the z component of the wave vector for the nth order harmonic ($K_\pm^{(n)} = k_x^{(n)}u_x + k_y^{(0)}u_y \pm k_z^{(n)}u_z$):

$$\begin{cases} k_z^{(n)} = +\sqrt{k^2 n_{hs}^2 - \left(k_{xy}^{(n)}\right)^2} \\ k_{xy}^{(n)} = +\sqrt{\left(k_x^{(n)}\right)^2 + \left(k_x^{(0)}\right)^2} \\ k_x^{(n)} = k_x^{(0)} + nk_x \\ k_x = \dfrac{\pi}{\Omega}\left|\sin\alpha_T\right| \end{cases} \tag{5}$$

where, $k = \frac{2\pi}{\lambda}$, λ is the wavelength of light in vacuum. The lower and the upper half-spaces are filled by a homogeneous, non-dissipative, dielectric medium of refractive index n_{hs}.

For $\alpha_T = 0$, all non-specular reflections and transmissions diminish ($n \# 0$) and only specular reflection and transmission of zero order harmonic will appear:

$$R^0_{\sigma\sigma'} = \left| \sum_{|n|\le N_t} r^{(n)}_{\sigma\sigma'} \right|^2,\ T^0_{\sigma\sigma'} = \left| \sum_{|n|\le N_t} t^{(n)}_{\sigma\sigma'} \right|^2,\ \sigma,\sigma' = L,R \tag{6}$$

In our calculations $N_t = 2$ was assumed, while higher N_t was also investigated and it was found out that the results are the same as that for $N_t = 2$ up to the accuracy of 10^{-6}.

Circular polarization selectivity of nth order harmonic for the graded chiral thin film is:

$$Selectivity^{(n)} = T^{(n)}_{LL} - T^{(n)}_{RR} \tag{7}$$

Since all non-specular transmission spectra for axial excitation state were less than 0.01 (1%), only the co-polarized transmission spectra T_{LL} and T_{RR} and circular polarization selectivity of the zero order harmonic were studied and reported in this work.

3. Results and discussions

For the purpose of simulation, it is assumed that a right-handed TiO_2 graded chiral sculptured thin film in its bulk state (rutile phase) with dielectric constants [40] given in Fig. 2 is formed, which occupies a space with the refractive index of n_{hs} (Fig. 1). The film thickness at a certain distance from the edge of the shadowing block is considered to be (d). In order to obtain the relative permittivity scalars $\varepsilon_{a,b,c}$, we used the Bruggeman homogenization formalism [41] with ellipsoidal form factors $\gamma^s_b = 2, \gamma^s_\tau = 20,\ \gamma^v_b = 2\gamma^v_\tau = 20$, [42] in the relative permittivity of the reference $\underline{\underline{\varepsilon}}_{\text{ref}}(\underline{r}) = \varepsilon_a \underline{u}_z \underline{u}_z + \varepsilon_b \underline{u}_x \underline{u}_x + \varepsilon_c \underline{u}_y \underline{u}_y$ ($\underline{u}_x$, $\underline{u}_y$ and $\underline{u}_z$ are Cartesian unit vectors). The homogenization process was carried out in 2 nanometer wavelength steps for each given frequency with respect to the refraction index of the TiO_2 at that frequency. In this way the dielectric dispersion function was implemented in the calculations. Hence, this method directly takes advantage of the experimental relative dielectric constant and avoids the use of simple dispersion model known as single-resonance Lorentzian model [43,44].

On the basis of Krause and Brett's experimental observation [25] the film thickness along a distance of 45 mm from the edge of the macroscopic shadowing block varies only about 1.5 μm (i.e., about 30 nm per mm distance or less than tenth of a complete pitch of chiral structures). By considering that the light diameter incident on the sample surface in the spectrophotometer is about 1 mm across, one can assume that in a given interaction region of the incident light the graded chiral sculptured thin film is a slanted chiral sculptured thin film and has constant structural parameters. It must be emphasised that the ellipsoidal form factors at different locations in the graded chiral sculptured thin films are different, however, in the present model we have assumed that the ellipsoidal form factor is unchanged at different locations. In further improving the model we will consider the role of variation of this factor at different locations. This should result in better agreements with the experimental results. In this paper the results of calculations for regions with more than 5 mm separation distance are reported. This choice of separation distance provides us with the opportunity to compare our theoretical results with Krause and Brett's experimental results [25], directly and the fact that two consecutive regions will have considerably different structural parameters.

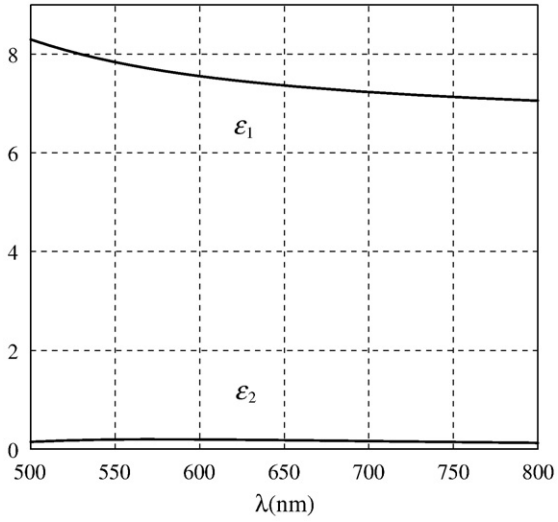

Fig. 2. The dielectric constant ($\varepsilon = \varepsilon_1 + i\varepsilon_2$, $\varepsilon_1 = n^2 - k^2$ *and* $\varepsilon_2 = 2nk$) of bulk TiO_2 (rutile phase), showing that the imaginary part is nearly zero in the wavelength region shown.

In order to be able to compare our results with those of Krause and Brett, the structural parameters of their reported work were needed. In their work d and Ω increased and α_T decreased as a function of increasing distance from the edge of the macroscopic shadowing block. The void fractions f_v and χ are constant for a given deposition angle.

In Fig. 3 the calculated results for the co-polarized transmission spectra T_{LL} and T_{RR}, and the circular polarization selectivity for a right-handed slanted chiral sculptured thin film in the axial excited state for a region at 50 mm distance from the edge of the shadowing block at a deposition angle of 70° are plotted. In Table 1 the experimental structural and deposition parameters adapted from Krause and Brett's work (using the data in Table 1 and Fig. 3 of Ref. [25]) for a graded chiral sculptured thin film deposited at 70° are given for different distances from the edge of the shadowing block. We used these parameters in our calculations.

The deposition angle of 70° was chosen on the basis of Sorge et al. [12] who reported the occurrence of the maximum of circular polarization selectivity at about this deposition angle. Outside the Bragg region, all reflections and transmissions show oscillations that correspond to the Fabry–Perot oscillations, which occur in a homogeneous medium because of the interference of reflected light from two surfaces of the medium. These reflections are affected by both thickness and the average of the refractive index of the medium [45]. Since the handedness of the chiral sculptured thin film and the polarization direction of the left-handed circularly plane wave are not the same, the interaction in the Bragg regime is low. Therefore, in the Bragg regime the left-handed circularly plane wave unlike the right-handed circularly plane wave is almost completely transmitted through the medium (Fig. 3-a). The maximum of the circular polarization selectivity is obtained at 694 nm which is in good agreement with the experimental result of Krause and Brett (690 nm) [25] (Fig. 3-b).

In Fig. 4, the calculated circular polarization selectivity spectra at different distances from the shadowing block, for a right-handed graded chiral sculptured thin film in axial excited state, produced at a deposition angle of 70° are depicted. In this figure in order to discriminate the spectra from each other, each spectrum is shifted to a higher level by 5%. The Bragg wavelengths used for obtaining Fig. 4 are given in Table 2.

Fig. 4 shows that the peak of the circular polarization selectivity (the location of appearance of the circular Bragg phenomenon) shifts towards shorter wavelengths (blue shift) by decreasing the distance from the shadowing block, while the intensity at its maximum is also reduced. This is due to decreasing of the structural period (because of reduction in film thickness), increasing of tilt angle of chiral nanocolumns (α_T) (see Table 1) and the fact that the film becomes anisotropic. Therefore, graded chiral sculptured thin film while

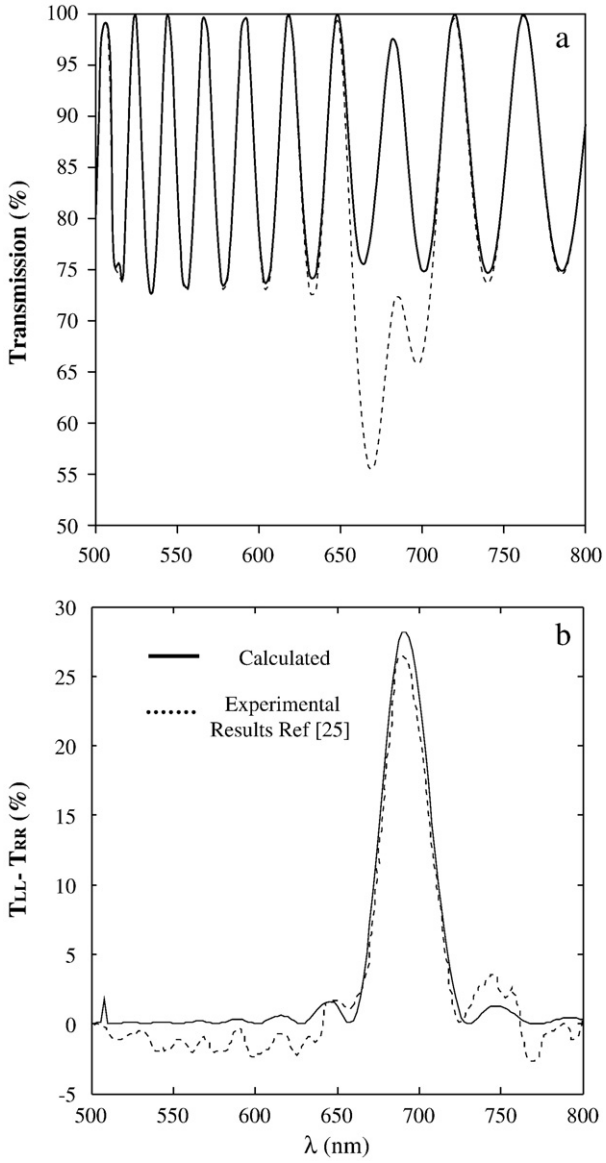

Fig. 3. a) T_{LL} and T_{RR} transmission spectra. b) Calculated difference in transmission spectra, for axially excited right-handed slanted chiral sculptured TiO_2 thin films at 50 mm from the edge of the shadowing block compared with that of experimental results from [25]. Deposition angle is 70° and $n_{hs}=1$.

possessing frequency tuneability is capable of changing the polarization of the incident light. Hence, it can simultaneously have filtering frequency and polarization selectivity properties of light.

In Fig. 5, the maximum circular polarization selectivity calculated at a distance of 50 mm from the edge of the shadowing block, for a

Table 1
The structural parameters for a graded chiral sculptured TiO_2 film produced at a deposition angle of 70° (adapted from Ref. [25]).

D (mm)	Ω(nm) $\Omega=\Omega^{BG}_{Exp}/\cos(\alpha_T)$	α_T (°)	χ (°)	d (nm)
50	200	6	37	18 Ω
35	192	11	37	18 Ω
20	186	15.5	37	18 Ω
15	177	17.3	37	18 Ω
10	173	17.5	37	18 Ω
5	160	18	37	18 Ω

D is the distance from the edge of the shadowing block; Ω^{BG}_{Exp} is the one half of the structural period from [25].

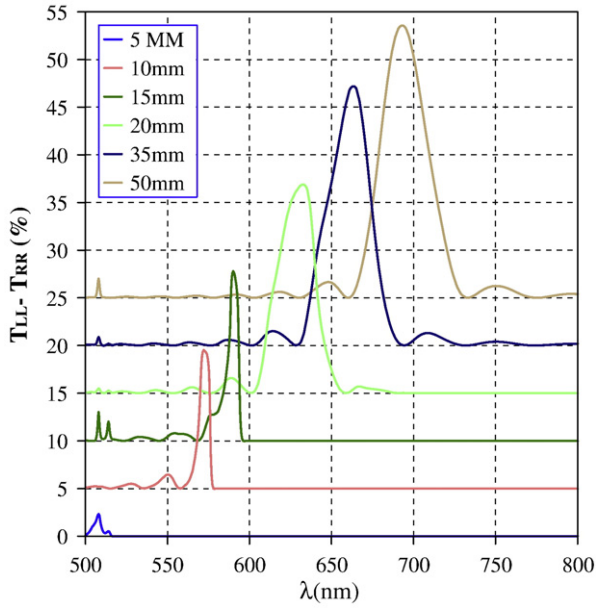

Fig. 4. Difference in transmission spectra for axially excited right-handed graded chiral sculptured TiO_2 thin films calculated at different distances from the edge of the shadowing block. Deposition angle is 70° and $n_{hs}=1$.

right-handed graded chiral sculptured thin film in axial excited state, produced at different deposition angles and according to the structural parameters given in Table 3 (adapted from Krause and Brett's [25] work), are plotted.

For a shadowing block of 20 mm height and the deposition angles of less than 70° and at a distance of 50 mm from the edge of the shadowing block, the tilt angle was assumed to be small, because at these deposition angles the shadowing length of the block is less than 50 mm. The rise angle for deposition angles greater or equal to 70° is in good agreement with Tait's law [46] but at lower deposition angles the existing relationships between the rise angle and deposition angle (reported for tilted columnar structure (i.e., tangent rule and the Tait's law) and not for helical structures) are not suitable, because at these angles the void fraction density in the sculptured helical thin film structure reduces and the structure consists of closely packed features. Hence, differentiation of individual chiral structures becomes more difficult. Therefore, in order to obtain results at deposition angles less than 70°, the rise angle was chosen as an adjusting parameter until the calculated results satisfied the experimental observations [25] (Table 3). It should be mentioned that the data given in Table 3 for the rise angle at deposition angles less than 70° (i.e., 65 and 60°) belong to the fitting of our calculations to Krause and Brett's data in Fig. 5, as neither numerical nor SEM results were present in Ref. [25] for these angles. On the other hand, the use of available relationships, such as tangent rule which is given for columnar thin films, proved to produce unacceptably large rise angles (i.e., 50 and 60°). The void fraction in thin films at deposition angles smaller than 75° can be obtained using the relationship $\rho=\rho_0\frac{2\cos(\alpha_d)}{1+\cos(\alpha_d)}$ (ρ and $\rho_0=3.9grcm^{-3}$ are the film and bulk densities, respectively) [25] and for deposition angles greater than 75° we used the experimental results reported in Ref. [47]. The results given in Fig. 5 are consistent with those obtained experimentally by Krause and Brett (see Fig. 9 in Ref. [25]) (the maximum of the circular polarization selectivity appears at 70°). At deposition angles

Table 2
λ_e^{Br} at different distances from the edge of the shadowing block.

D (mm)	5	10	15	20	35	50
λ_e^{Br}(nm)	510	572	590	632	664	694

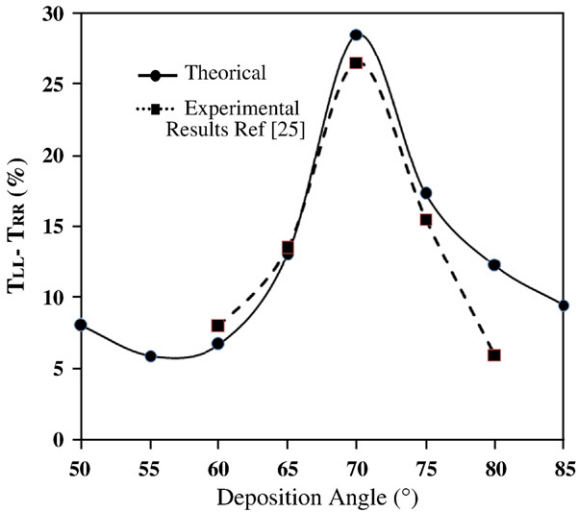

Fig. 5. Maximum selectivity calculated at 50 mm from the edge of the shadowing block for different deposition angles. $n_{hs}=1$.

smaller than 70°, according to the 5th column in Table 3 the void fraction decreases and the film becomes almost isotropic. Hence, at these deposition angles due to reduction of the intensity in the circular Bragg phenomenon the circular polarization selectivity decreases, too. At deposition angles greater than 70°, the void fraction increases, the chirality of the film diminishes and the scattering increases, resulting in lower circular polarization selectivity [48].

Bragg wavelengths calculated for a different angle of incidence at a distance of 50 mm from the edge of the shadowing block and used for obtaining the results in Fig. 5 are given in the last column of Table 3.

In Fig. 6(a–c), the spectra of circular polarization selectivity obtained from our calculation for a right-handed graded chiral sculptured TiO_2 thin film in axial and non-axial excited states at 70° deposition angle for three different distances from the shadowing block ($D=10, 20$ and 50 mm) are depicted. It can be observed that the circular polarization selectivity for non-axial excitation state is higher than that for axial excitation at any given distance from the edge of the shadowing block. This is due to the fact that in non-axial excitation state the angle of incidence of the light on the film (θ_{inc}) is chosen to be the same as α_T of nano-columns. This choice increases the intensity of the circular Bragg phenomenon which results in increased circular polarization selectivity. Of course at distances far away from the shadowing block the difference seen in Fig. 6 diminishes due to the fact that the film structure becomes isotropic and the nano-columns grow normal to the substrate surface. Hence, if higher circular polarization selectivity at distances close to the shadowing block is required, the incident light angle on the film (θ_{inc}) should be chosen to be similar to α_T of the nano-columns at that distance. This selection of the angle of

Table 3
The structural parameters for slanted chiral sculptured TiO_2 films produced at different deposition angles. Distance from the edge of the shadow block is $D=50$ mm and thickness is 18 Ω. (adapted from Ref. [25]).

Deposition angle (°)	Ω (nm) $\Omega=\Omega^{BG}_{Exp}/\cos(\alpha_T)$	α_T (°)	χ (°)	f_v (%)	λ_e^{Br} (nm) calculated
50	184	0.1	40	28	794
55	188	0.1	40	33	778
60	195	0.1	39	39	762
65	197	0.1	38	45	726
70	200	6	37	53	694
75	227	20	35	62	648
80	244	22	32	68	628
85	253	25.5	30	75	572

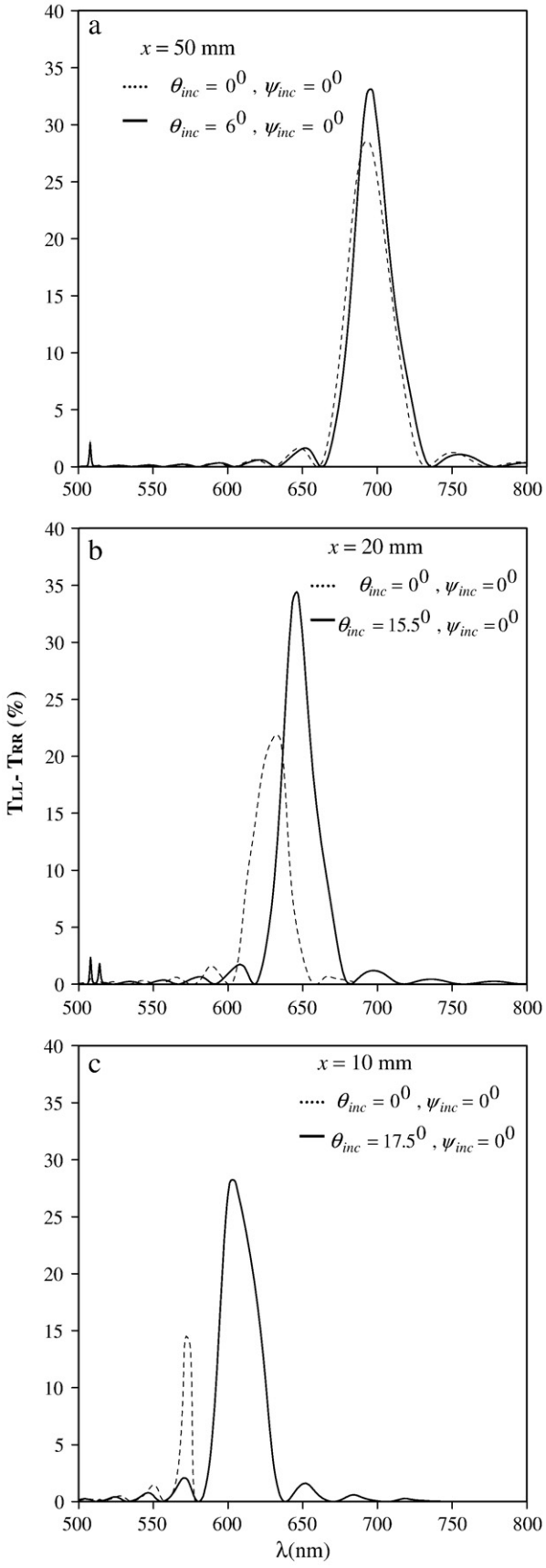

Fig. 6. Polarization selectivity spectra of a right-handed graded chiral sculptured TiO_2 thin film in axial ($\theta_{\text{inc}}=0°$) and non-axial excited states at 70° deposition angle for three different distances from the shadowing block. a) $x=10$ mm, b) $x=20$ mm, and c) $x=50$ mm). $n_{hs}=1$.

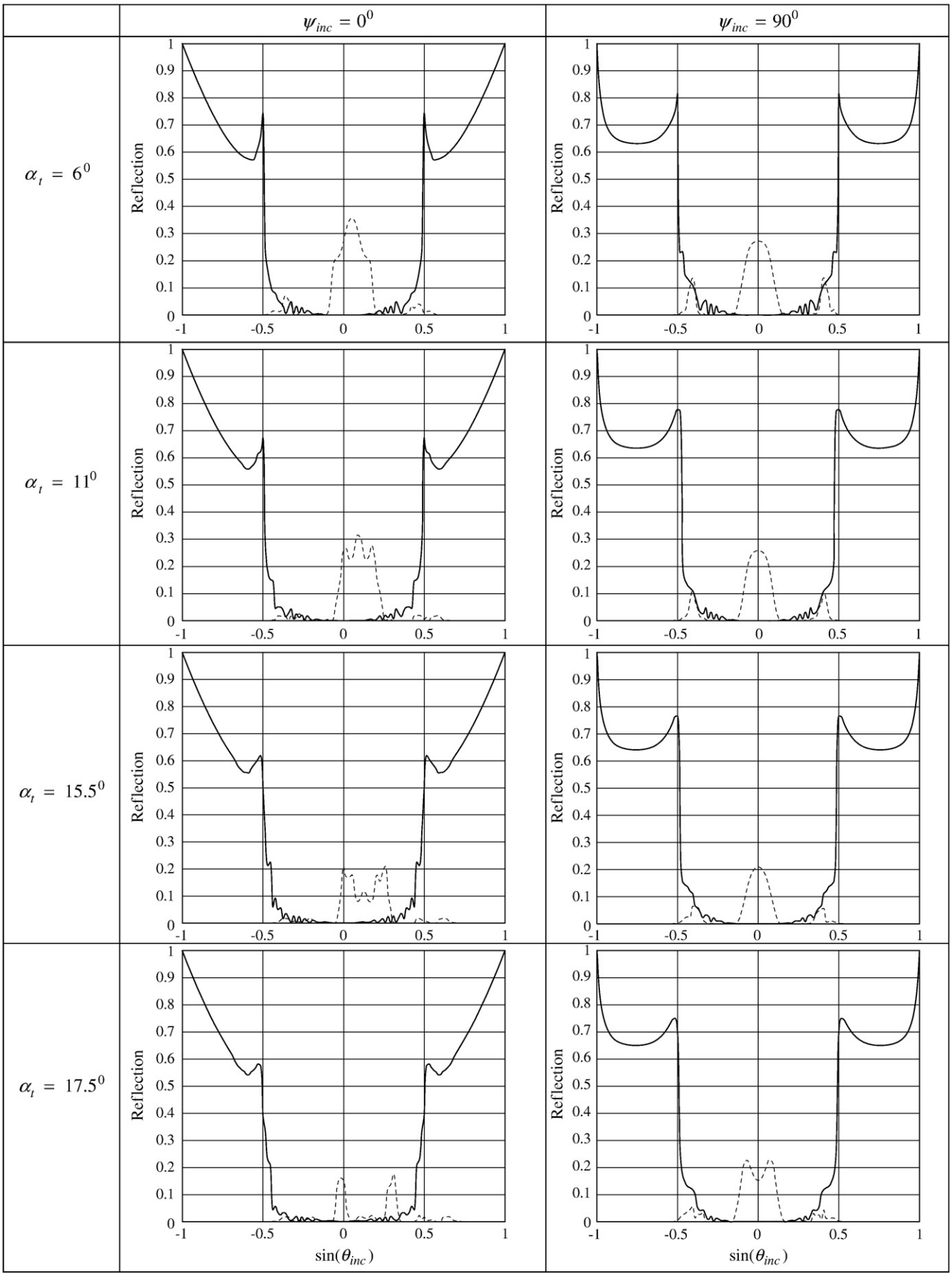

Fig. 7. Reflection spectra for a right-handed graded chiral sculptured TiO_2 thin film. Deposition angle is 70° and $n_{hs} = 3.5$. Dashed curve is R_{RR}^{-2} and solid curve is R_{RR}^{0}.

incidence causes a blue shift in axial excited state and a red shift in non-axial excited state.

In Fig. 7, the circular reflection spectra R_{RR}^{-2} and R_{RR}° for a right-handed graded chiral sculptured TiO_2 thin film in non-axial excited states produced at 70° deposition angle for four different distances from the shadowing block ($\alpha_T = 6°$, 11°, 15.5° and 17.5°) and for the Bragg wavelength given in Table 2 (Bragg wavelength is the wavelength that is obtained from the calculations in the axial excitation state) are plotted. From the comparison of R_{RR}^{-2} spectra in $\Psi_{inc} = 0°$ and $\Psi_{inc} = 90°$ plots it can be deduced that at $\Psi_{inc} = 90°$ the spectra are symmetric, which is due to anomaly effects (Rayleigh-Wood anomalies phenomenon) on circular Bragg phenomenon. It should be mentioned that at $\Psi_{inc} = 0°$ the intensity and location of the circular Bragg phenomenon depends on α_T.

From the comparison of R_{RR}° spectra in $\Psi_{inc} = 0°$ and $\Psi_{inc} = 90°$ plots (Fig. 7) it can be deduced that the total reflection regime ($|\sin\theta_{inc}| \in [0.55, 1)$ is insensitive to α_T of nano-columns or the different distances from the edge of the shadowing block and hence to the filtering frequency property. In addition, it is being reported that the total reflection regime does not depend on the handedness of the film [23].

Fig. 1 compares the results obtained for the n_{ave} from the Bragg wavelength, $\lambda^{Bragg} = n_{ave}(2\Omega)\cos(\alpha_T)$ [49] and the values obtained for n_{ave} from calculations of n_c and n_d as [50]:

$$n_c = \varepsilon_c^{1/2}, \tag{8}$$

$$n_d = \left(\frac{\varepsilon_a \varepsilon_b}{\varepsilon_a \cos^2\chi + \varepsilon_b \sin^2\chi}\right)^{1/2}, \tag{9}$$

$$n_{ave} = \frac{n_c + n_d}{2}, \tag{10}$$

for a right-handed graded chiral sculptured TiO_2 thin film in an axial excited state at different deposition angles and at distance of 50 mm from the edge of the shadowing block. The small values of n_{ave} obtained at higher deposition angles are due to the increased void fraction.

The results presented in Fig. 1 are consistent with those of Krause and Brett [25]. The theoretical results in this work show the same behavior as those of the experimental work. The small deviation at deposition angles greater than 75° (Figs. 5 and 8) could be due to the fact that the following phenomena are not included in our calculations: 1) the strong scattering from the surfaces of the nano-structures at these angles, 2) disappearance of helical columns with increasing film thickness and increase of their diameter, 3) existence of two different media above (vacuum) and underneath (substrate) the film, 4) more precise data (measurements) for structural parameters, 5) instrumental (experimental) uncertainties, and other parameters. The inclusion of the above phenomena in the calculations should enhance the results.

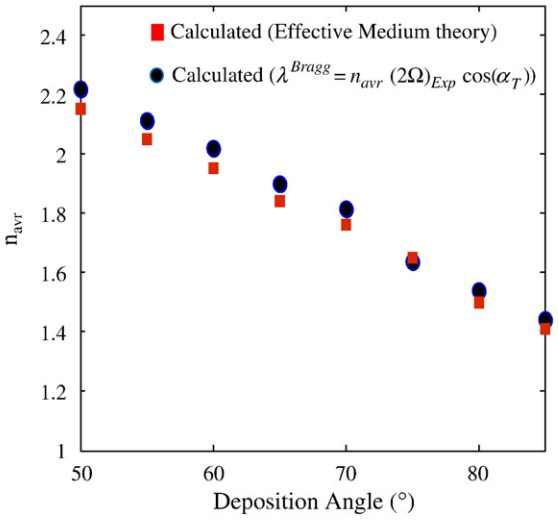

Fig. 8. The n_{ave} obtained from the Bragg wavelength, $\lambda^{Bragg} = n_{ave}(2\Omega)\cos(\alpha_T)$ compared with the results of the effective medium theory.

4. Conclusions

We used the rigorous coupled wave analysis (RCWA) method in conjunction with the Bruggeman homogenization formalism to calculate the co-polarized reflection and transmission spectra and the circular polarization selectivity for a right-handed graded chiral sculptured TiO_2 thin film in both axial and non-axial excitation states. The influence of structural and deposition parameters, namely, void fraction, structural period, tilt angle, deposition angle, and distance from the edge of the shadowing block on these spectra was studied. A good agreement between our theoretical calculations and the experimental results reported by Krause and Brett [25] is achieved. It is deduced that in order to observe high circular polarization selectivity at close distances to the edge of the shadowing block, the angle of incidence of light θ_{inc} must be equal to α_T of the nano-columns. This work has indicated that the RCWA can successfully be used to characterize and predict the behavior of the graded chiral sculptured thin films.

Acknowledgements

This work was supported by the University of Tehran and the University of Qom.

References

[1] K. Robbie, J.C. Sit, M.J. Brett, J. Vac. Sci. Technol. B 16 (1998) 1155.
[2] S.R. Kennedy, M.J. Brett, J. Vac. Sci. Technol. B 22 (2004) 1184.
[3] V.C. Venugopal, A. Lakhtakia, Proc. R. Soc. London A 456 (2000) 125.
[4] J. Wang, A. Lakhtakia, J.B. Geddes III, Optik 113 (2002) 213.
[5] V.C. Venugopal, A. Lakhtakia, in: O.N. Singh, A. Lakhtakia (Eds.), Electromagnetic Fields in Unconventional Materials and Structures, Wiley, New York, 2000, p. 151.
[6] V.C. Venugopal, A. Lakhtakia, Eur. J. Phys. Appl. Phys. 10 (2000) 173.
[7] M.D. Pickett, A. Lakhtakia, J.A. Polo, Optik 115 (2004) 393.
[8] M.W. McCall, A. Lakhtakia, J. Mod. Opt. 47 (2000) 973 corrections: 50 (2003) 2807.
[9] M.W. McCall, Math. Comput. Modell. 34 (2001) 1483.
[10] F. Babaei, H. Savaloni, Opt. Commun. 278 (2007) 221.
[11] F. Babaei, H. Savaloni, Opt. Commun. 278 (2007) 321.
[12] J.B. Sorge, A.C. van Popta, J.C. Sit, M.J. Brett, Optics Express 14 (2006) 10550.
[13] A. Lakhtakia, M.W. McCall, J.A. Sherwin, Q.H. Wu, I.J. Hodgkinson, Opt. Commun. 194 (2001) 33.
[14] I. Hodgkinson, Q.H. Wu, B. Knight, A. Lakhtakia, K. Robbie, Appl. Opt. 39 (2000) 642.
[15] Q. Wu, I.J. Hodgkinson, A. Lakhtakia, Opt. Eng. 39 (2000) 1863.
[16] F. Wang, A. Lakhtakia, R. Messier, Eur. Phys. J. Appl. Phys. 20 (2002) 91 corrections: 24 (2003) 91.
[17] W.C. Meecham, J. Appl. Phys. 27 (1956) 361.
[18] D. Maystre (Ed.), Selected Papers on Diffraction Gratings, SPIE Press, Bellingham, WA, 1993.
[19] F. Wang, A. Lakhtakia, Opt. Commun. 215 (2003) 79.
[20] F. Wang, A. Lakhtakia, Opt. Commun. 235 (2004) 107.
[21] I.J. Hodgkinson, Q.h. Wu, A. Lakhtakia, M.W. McCall, Opt. Commun. 177 (2000) 79.
[22] I.J. Hodgkinson, Q.H. Wu, K.E. Thorn, A. Lakhtakia, M.W. McCall, Opt. Commun. 184 (2000) 57.
[23] F. Wang, PhD Thesis, Pennsylvania State University, 2005.
[24] Y. Cui, MSc Thesis, Queen's University, 2005.
[25] K.M. Krause, M.J. Bret, Adv. Funct. Mater. 18 (2008) 3111.
[26] E. Nicolescu, M.J. Escuti, Proc. SPIE 6654 (2007) 665405.
[27] W.D. Shen, M. Cathelinaud, M. Lequime, F. Charpentier, V. Nazabal, Opt. Express 16 (2008) 373.
[28] N. Sedoglavich1, J.C. Sharpe, R. Künnemeyer, S. Rubanov, Opt. Express 16 (2008) 5832.
[29] S.A. Jewell, P. Vukusic, N.W. Roberts, New J. Phys. 9 (2007) 99.
[30] P. Vukusic, R. Kelly, I. Hooper, J. R. Soc. Interface 6 (2009) S193.
[31] P. Vukusic, J. Roy Sambles, Nature 424 (2003) 852.
[32] A. Piegari, J. Bulir, Appl. Opt. 45 (2006) 3768.
[33] D.W. Dobbs, I. Gershkovich, B.T. Cunningham, Appl. Phys. Lett. 89 (2006) 123113.

[34] B.S. Krusor, D.B. Fenner, D.K. Biegelsen, R.D. Yingling, R.D. Bringans, J. Vac. Sci. Technol., B B 8 (1989) 172.
[35] Q. Wang, H. Moutinho, B. To, J. Perkins, D. Ginley, H.M. Branz, L.R. Tessler, D. Han, Proc. Mater. Res. Soc. Symp. A 762 (2003) A9.1.1.
[36] M. Born, E. Wolf, Principles of Optics, 7th Ed.Cambridge University Press, Cambridge, 1999.
[37] A. Thelen, J. Opt. Soc. Am. 53 (1963) 1266.
[38] R.M.A. Azzam, N.M. Bashara, Ellipsometry and Polarised Light, Amsterdam, North Holland, 1977.
[39] M.G. Moharam, T.K. Gaylord, J. Opt. Soc. Am. 71 (1981) 811.
[40] E.D. Palik, Handbook of Optical Constants of Solids, Acadamic Press, New York, 1985.
[41] J.A. Sherwin, A. Lakhtakia, Math. Comput. Modell. 34 (2001) 1499 corrections, 35 (2002) 1355.
[42] J.A. Sherwin, A. Lakhtakia, I.J. Hodgkinson, Opt. Commun. 209 (2002) 369.
[43] F. Babaei, H. Savaloni, J. Mod. Opt. 55 (2008) 1845.
[44] F. Babaei, H. Savaloni, J. Mod. Opt. 55 (2008) 2347.
[45] E. Hecht, Optics, 4th EdAddison Wesley, San Francisco, 2002.
[46] R.N. Tait, T. Smy, M.J. Brett, Thin Solid Films 226 (1993) 196.
[47] F. liu, C. Yu, L. Shen, J. Barnard, G.j. Mankey, IEEE Trans. Magn. Vol. 36 (September 2000) (No. 5).
[48] A.C. van Popta, J.C. Sit, M.J. Brett, Appl. Opt. 43 (2004) 3632.
[49] F. Wang, A. Lakhtakia, R. Messier, Eur. Phys. J. AP 20 (2002) 91 (corrections: 24 (2003)91).
[50] M.W. McCall, A. Lakhtakia, J. Mod. Opt. 51 (2004) 111.